

Continuum Terahertz Radiation Detection Using Membrane Filters

P. Kaufmann*, A.S. Kudaka, M.M. Cassiano,
A.M.Melo
CRAAM – Escola de Engenharia
Universidade Presbiteriana Mackenzie
São Paulo, Brazil

R. Marcon
Instituto de Física “Gleb Wataghin”
Universidade Estadual de Campinas
Campinas, Brazil

A. Marun, P. Pereyra, R. Godoy, H. Levato
Complejo Astronómico El Leoncito, CONICET
San Juan, Argentina

A.V. Timofeevsky, V.A. Nikolaev
Tydex J.S. Co, St. Petersburg, Russia

*also at CCS –Universidade Estadual de Campinas, Campinas, Brazil

Abstract— Technology of remote sensing in the terahertz range (frequency interval arbitrarily set between 0.1 – 30 THz) is the object of considerable development efforts addressed to a number of new civilian and military applications. Technical challenges appear in the THz sensing of temperature differences above an existing hot surface target, such as radiation patterns produced by high energy electrons in laboratory accelerators, and thermal differentiated structures in the solar disk in space. The efficient suppression of radiation in the visible and near infrared (set arbitrarily for wavelengths $< 10 \mu\text{m}$) is an essential requirement. An experimental setup has been prepared for testing at room temperature THz materials and detectors, aiming the detection of solar radiation. A custom-made detector consisted in a room-temperature micro-bolometer INO camera with HRFZ-Si window. The THz transmission of two “low-pass” membranes were tested for black body temperatures ranging 300-1000 K: Zitex G110G and TydexBlack. It has been demonstrated that both are effective suppressors of radiation at wavelengths $< 15 \mu\text{m}$, with the first one exhibiting a small radiation excess, that may be attributed to small visible and NIR allowance. We describe optical setups prepared to detect solar radiation, consisting in a microbolometer camera preceded by a photon pipe, low-pass membrane and band-pass resonant metal mesh, placed at the focus of the 1.5 m reflector for submillimeter waves (SST) at El Leoncito, Argentina Andes.

Keywords—terahertz materials; terahertz transmission; terahertz sensors; terahertz filters

I. INTRODUCTION

Technologies for photometry and imaging in the THz range (arbitrarily 0.1 – 30 THz) are in full expansion for a variety of new and unique applications in different civil and military areas presenting a number of distinctive advantages on the well known microwaves or near-infrared technologies. THz radiation propagates well through cloth, dust and fog [1]-[3]. Sensing in this range is proving to be particularly useful to

This research was partially funded by Brazilian agencies CNPq – INCT NAMITEC, FAPESP, Mackpesquisa and Argentina agency CONICET

determine internal characteristics of materials, in the search for drugs, mines and explosive materials. New biological and medical THz imaging applications are far reaching. Aerospace THz remote sensing applications include new approaches to determine atmospheric inhomogeneities and cloud characteristics [4]-[6].

Photometry and imaging at THz frequencies have important application in the diagnostics of radiation produced by high energy electrons, observed in laboratory accelerators [7] and by thermal and non-thermal space plasmas [8][9]. We are currently developing subsystems needed for the assembly a THz photometer/imager to be used in solar flare observations at discrete frequencies from the ground, in the atmosphere transparency 0.4; 0.67 and 0.86 THz windows at a high altitude site, and from space at 3 THz. One essential requirement to perform these measurements is the effective suppression of input visible and near infra-red (NIR) radiation. This can be obtained using a number of THz low-pass filters [4]. We present here the experimental arrangements made to measure the transmission of materials commercially available: Zitex G110 G [10] and BlackTydex [11]. Optical setups are shown for solar observations using the same laboratory THz photometer arrangement.

II. THE EXPERIMENTAL ARRANGEMENT

The tests were carried out by collimating a radiating blackbody (made with a nichrome resistor) at an INO MMICII V2 camera focal plane array of vanadium oxide micro-bolometers, according to the schematic arrangement shown in Figure 1. The 0.15 m diameter concave mirror was adjusted to produce a real image at the camera FPA (without any lens). Resistor temperatures were measured by a coupled thermopair. The low pass filters were placed in front of FPA:

TydexBlack and Zitex G 110. The range of temperatures were typically from ambient (about 300 K) to 1000 K. Figure 2 illustrate the actual assembly.

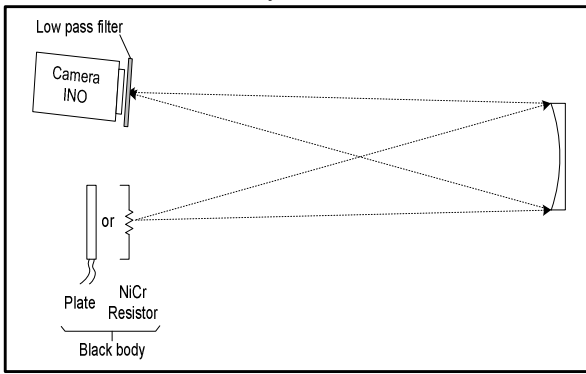


Figure 1. Principle of the experimental setup



Figure 2. INO camera with TydexBlack THz filter placed in front of the FPA (left). At right the nichrome heated resistor, the 0.15 m concave reflector in the background aligned to form its image in the camera FPA (located behind the protecting surface, at the left of the picture).

III. THE THz LOW-PASS FILTER MEMBRANES

The Zitex G110 film (0.25 mm thickness, sintered Teflon with 1-2 μm pore sizes) is known as an effective suppressor of radiation with wavelengths shorter than 15 μm , where the measured transmission is nearly zero [10]. See Figure 3.

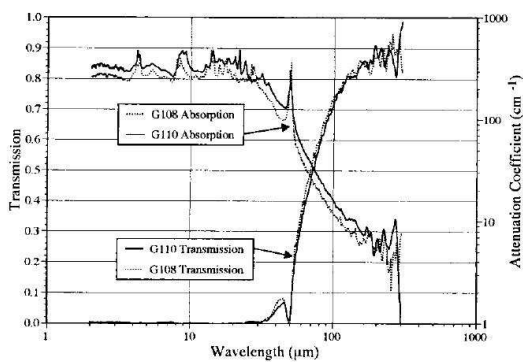


Figure 3. Zitex G110 transmission and absorption [10]

The transmission of this membrane was recently re-measured by Tydex Company, at St. Petersburg, Russia, with results shown in Figure 4. Although confirming the Zitex

G110 transmittance in the THz range, careful measurements taken in the visible-near infrared ($< 15 \mu\text{m}$) range revealed a small amount of power transmission, shown in Figure 5, corresponding approximately to about 0.3 % of the power in the visible-NIR. This amount may become significant in relative power since blackbody radiation at temperatures ranging 300-1000 K produce nearly 20 times more power in the visible-NIR compared to the power in the $> 15 \mu\text{m}$ range.

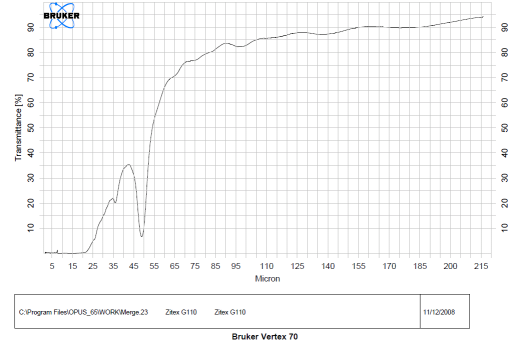


Figure 4. Zitex G110 transmittance as measured at Tydex laboratory

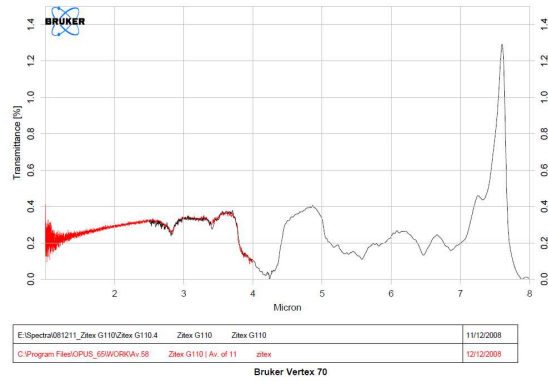


Figure 5. Transmittance of Zitex G110 in the near infrared, as measured at Tydex laboratory

The alternate THz low-pass filter considered was the TydexBlack membrane, produced by Tydex company [11]. The TydexBlack THz transmittance is shown in Figure 6.

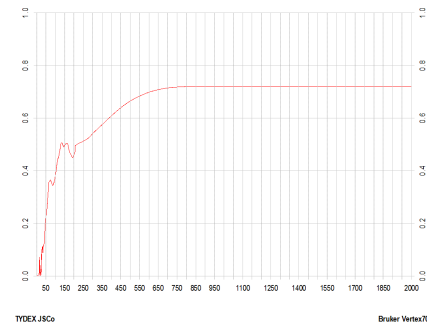


Figure 6. TydexBlack THz transmittance [11]

The visible - near infrared transmittance of TydexBlack, shown in Figure 7, is considerably smaller compared to Zitex

G110 (Figure 5). The power transmission in the NIR is \ll 0.05% (compared to the 0.2% measured for Zitex G110).

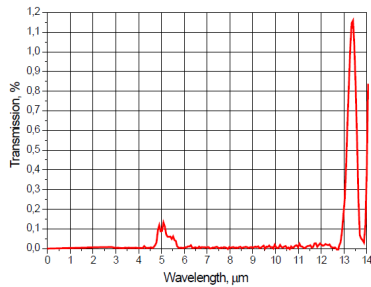


Figure 7. The TydexBlack NIR transmittance is considerably smaller compared to Zitex G110 (Figure 5) [12]

IV. RESPONSE TO BLACK BODY RADIATION

The nichrome resistor emission may be assumed as being close to an ideal black body radiator. The resistor image occupied nearly 70 % of the camera FPA. We selected the Region Of Interest (ROI) over the area in the frame filled by the heated resistor. All pixels readings on the ROI were added and averaged for every frame reading, quoted in camera reading units. Several sets of measurements were taken, for temperatures ranging from ambient to about 900 K. One series of measurements are summarized in Figure 8.

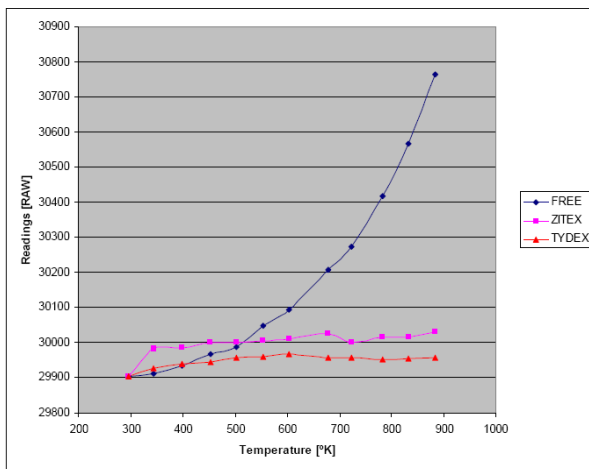


Figure 8. INO camera response to the temperature of the black body (resistor) collimated on the focal plane array, free path (blue), and with low pass filters interposed (pink and red)

The camera response with the low pass filters interposed in front of the FPA was considerably reduced. Another series of measurements using TydexBlack membrane are zoomed in Figure 9. The fluctuations of data points can be attributed to measurement fluctuations (of about ± 1 reading unit), since they were taken with short time integration (30 frames/s), at the limit sensitivity. It can be noted that the camera readings

with Zitex G110 low pass filter interposed is about 20-40 reading units above the TydexBlack readings, for the whole range of temperatures. This effect was repeatedly observed for all series of measurements. It might correspond to the fraction of power in the visible-NIR transmitted by Zitex G110 (see Figure 5).

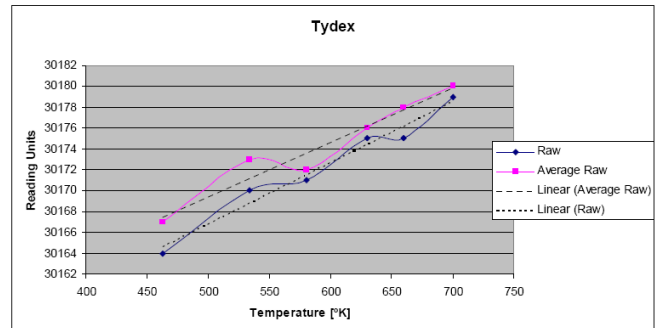


Figure 9. Another independent set of measurements for TydexBlack interposed. The “average raw” plot is for several data readings averaged at a same temperature. The “fluctuations” are representative of the uncertainties of the measurements

To evaluate the effective low pass filtering of radiated power in the approximate $> 15 \mu\text{m}$ range, we shall compare to calculated black body variation in radiant power for a given temperature change at a given reference temperature. There are several website readily available for quick calculations [12]. In the higher temperatures the measurements are better defined. Taking the measurements at 783 K and 883 K, we can predict the increase in radiant power within the band (band radiance):

$$\Delta P(0.5-1000) \approx 4188.3 \text{ W/m}^2/\text{sr}, \text{ for the wavelength range of } 0.5 \text{ to } 1000 \mu\text{m} \text{ (i.e., without low pass filter)}$$

$$\Delta P(15-1000) \approx 76.5 \text{ W/m}^2/\text{sr}, \text{ for the wavelength range of } 15 - 1000 \mu\text{m} \text{ (with low pass filter).}$$

The predicted ratio of power increase for a black body heated from 783 K to 883 K is close to 55. From Figures 8 and 9, powers are proportional to the square of the camera reading units. The measured power increase is proportional to the difference of squares of reading units for 783 K and 883 K. We obtain the ratio for power increases for free transmission to low pass filter transmission (data taken from the best fit line) of about 108 (for BlackTydex) and of 55 (for Zitex G110). The difference in the attenuation factors might be acceptable, in view of the fluctuations in the camera reading units. This result is qualitatively close to the predicted ratio of power increase.

We conclude that both Zitex G110 and TydexBlack low pass filters effectively suppress the short NIR and visible

radiation. The Zytex G110 filter, however, appear to allow a small excess transmission in the whole range of temperatures.

V. SETUP FOR BOLOMETER SOLAR OBSERVATION

There were mechanical developments made at CASLEO to place the INO camera and filters at the focus of the solar submillimeter-wave telescope (SST) 1.5 –m reflector, located at El Leoncito, 2550 m altitude, Argentina Andes [13]. Two configurations were prepared: (a) Prime focus, or Newtonian (illustrated in Figure 10); (b) Nasmyth configuration (adding a tertiary flat mirror to the Cassegrain setup).

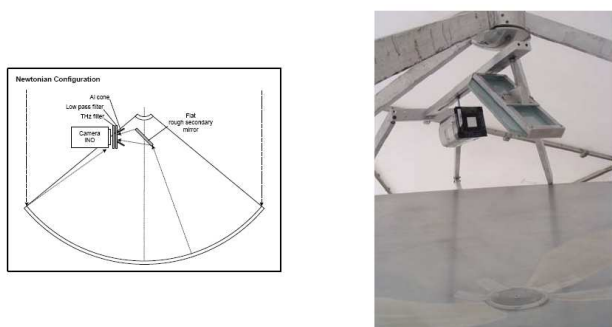


Figure 10. The primary focus configuration design (left), and installation (right)

The flat secondary mirror has a aluminized rough surface to diffuse and further minimize the visible and NIR radiation as described by Kornberg et al. [14]. A photon trap parabolic cone was added to enhance the total solar disk radiation into the detector FPA.

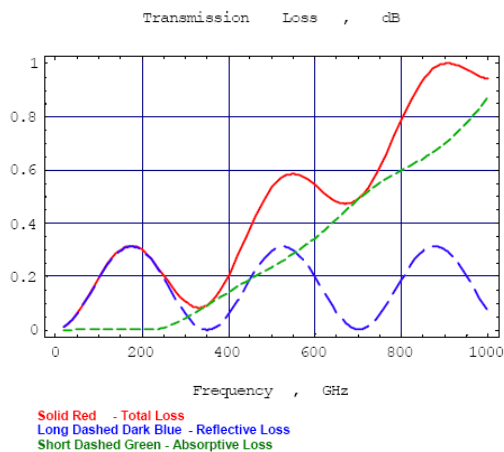


Figure 11. M12-81-8000 ESSCO Radome GoreTex™ Membrane losses [15]

The SST radome losses for smaller THz frequencies are shown in Figure 11. It indicates that the membrane transmission becomes sufficiently good for frequencies less than about 0.8 THz.

VI – BOLOMETRIC DETECTION LIMITS USING THE 1.5-M REFLECTOR ANTENNA.

A. Atmosphere attenuation factors

The best values for atmosphere attenuation measured at El Leoncito at 0.4 THz range 0.7- 1.0 nepers [16]. For qualitative estimate we may adopt for low opacity days an optimum optical depth of $\tau = 0.8$ nepers at El Leoncito. For these days we may assume a model extrapolation giving $\tau = 1.5$ nepers for the “windows” at 0.67 THz and 0.85 THz. The solar disk temperature in these frequencies is close to approximately 5000 K [18]. For $\tau = 0.8$ nepers at 0.4 THz, elevation angle $H = 35^\circ$, the brightness is reduced by a factor $\exp[\tau/\sin H] = 8$. Beam efficiency of 0.5 might be arbitrarily assigned, resulting in a reduction final factor of about 8. We expected solar antenna temperature of about 620 K. For $\tau = 1.5$ nepers at 0.67 and 0.85 THz, assuming the same elevation angle and beam efficiency, adding the attenuation due to the radome, we may expect solar antenna temperatures of the order of 225 K at 0.67 THz and of 140 K at 0.85 THz.

B. Detectability for FOV smaller than the solar disk

The measurements performed in section IV indicated the INO camera response of about 20 K per reading unit, for $\lambda > 15 \mu\text{m}$, averaging pixels over a large ROI. These measurements were obtained collimating a black-body radiation source through a 0.15 m diameter concave reflector. The use of the metal mesh resonant filters [18] interposed to the low pass filter further reduces the available power at the center frequencies $\pm 10\%$ band-pass by a factor of about 100. On the other hand, it is necessary to scale the measurements with the camera placed at the SST focus, taking into account a gain factor, corresponding to the gain ratio of SST 1.5 m reflector with respect to the 0.15 m collimating reflector gain at the corresponding frequencies. It can be shown that the SST has a gain roughly 100 bigger than the 150 mm reflector used in the laboratory tests. It roughly compensates the power limited within the band-pass set by the metal mesh filters.

Therefore, for the above good atmosphere transmission conditions one might expect to obtain about 30 reading units at 0.4 THz; 10 reading units at 0.67 THz and 7 reading units at 0.85 THz. We predict that 3 sigma detection of the solar disk should be possible with small time constant (0.2 seconds) at 0.4 THz. Considerably longer integration times might be needed to detect the solar disk at 0.67 and at 0.85 THz.

C. Detection of temperature enhancement of sources smaller than the FOV

The minimum detectable solar flux for a burst source smaller than the field of view can be derived from the well known equation:

$$\Delta S = 2 k \Delta T_a / A_e \text{ Wm}^{-2}\text{Hz}^{-1}$$

Where k is the Boltzmann constant, ΔT_a is the detectable temperature difference and A_e is the aperture effective area. The camera operating with 5/second cadence provided r.m.s. of 1.5 reading units, which correspond to about 20 K in antenna temperature. We remind that the 1.5 m antenna gain/0.15 m ratio equals approximately the power reduction within the 10% band-pass, at frequencies centered on 0.4, 0.67 and 0.85 THz. Therefore we may assume that 3 sigma detection levels equals approximately 4.5 reading units, or 90 K. Substituting in the above equation, for 20% aperture efficiency for the 1.5 m reflector (at 0.4 THz for coherent radiation) [13], we obtain a 3 sigma flux detection of about $100 \cdot 10^{-22} \text{ Wm}^{-2}\text{Hz}^{-1}$, or 100 solar flux units, at 0.4 THz, with 0.2 s time constant.

We may tentatively predict the SST antenna aperture efficiency for higher frequencies using the well known Ruze equation [19], valid for coherent detectors at the focal plane. Extrapolating from the 20% efficiency at 0.4 THz [13] we obtain estimates of 4% and 1% at 0.67 and 0.85 THz respectively, which would imply in flux density lower detection limits with 0.2 s time constant of about 500 and 2000 SFU, respectively.

ACKNOWLEDGMENTS

We acknowledge the technical support received from J.L. Aballay, E. Alvarez, G. Fernandez, H. Molina, H. Ruartes at Complejo Astronomico El Leoncito, San Juan, Argentina, and from E.C. Bertolucci and M.B. Zakia at CCS, Unicamp, Campinas, Brazil.

REFERENCES

- [1] Harris, D.C., "Materials for infrared windows and domes", SPIE Optical Engineering Press, Washington, USA, C, 1999.
- [2] Siegel P. H., "THz Technology: An Overview", International Journal of High Speed Electronics and Systems, vol. 13, n°2, 1-44, 2003.
- [3] Mlynczak, M., Johnson, D., Bingham, G., et al., "Far-Infrared Spectroscopy of the Troposphere (FIRST) project", Proceedings of Geoscience and Remote Sensing Symposium, vol. 1, 512, 2003.
- [4] Sherwin M. S., Schmuttenmaer C. A., Bucksbaum P. H., Proceedings of DOE-NSF-NIH Workshop on Opportunities in THz Science, Arlington, VA, 2004.
- [5] Kinch, M.A., "Infrared detector materials", SPIE Optical Engineering Press, Vol. TT76, Washington, USA, DC, 2007.
- [6] Strabala K. I., Ackerman S. A. and Menzel W. P., "Cloud Properties inferred from 8–12- μm Data", *Journal of Applied Meteorology*, **33**, 2, 212, 1994.
- [7] Williams, G. P., "FAR-IR/THz radiation from the Jefferson Laboratory, energy recovered linac, free electron laser", *Rev. Sci. Instrum.* **73**, 1461-1463, 2002.
- [8] Kaufmann, P. and Raulin, J.-P., "Can microbunch instability on solar flare accelerated electron beams account for bright broadband coherent synchrotronmicrowaves?", *Phys. Plasmas* **13**, 070701-070701-4, 2006.
- [9] Klopff, J. M., in *Ist SMESE Workshop*, 10-12 March, Paris, France, 2008.
- [10] Benford, D.J., Gaidis, M.C., and Kooi, J.W., "Optical properties of Zitex in the infrared to submillimeter", *Applied Optics* **42**, 5118-5122, 2003.
- [11] www.tydex.ru, Tydex JSCo, Technical Note on THz materials and components, 2008.
- [12] http://spectralcalc.com/blackbody_calculator/blackbody.php, GATS, Inc., Blackbody radiance,
- [13] Kaufmann, P., et al., "New telescopes for ground-based solar observations at submillimeter and mid-infrared", *Proc. SPIE* **7012**, 70120L-1-8, 2008.
- [14] Kornberg, M. et al., "Rough Mirrors for the THz frequency range", *Proc. MOMAG 2008 – 13th SBMO and 8th CBMAG*, Florianópolis, SC, Brazil, 365-367, 2008.
- [15] ESSCO, West Concord, MA, USA, private communication, 2008.
- [16] Melo, A.M. et al., "Submillimeter-wave Atmospheric Transmission at El Leoncito, Argentina Andes", *IEEE Trans Ant. Propagat.* **53**, 1528, 2005.
- [17] Gezari, D.Y., Joyce, R.R. and Simon, M., "Measurement of the Solar Brightness Temperature at 345 , 450 and 1000 micrometers", *Astron.Astrophys.* **26**, 409-411, 1973.
- [18] Melo, A.M. et al., "Metal mesh resonant filters for terahertz frequencies", *Applied Optics* **47**,6064-6069, 2008.
- [19] Ruze, J., "The effect of aperture errors on the antenna radiation pattern", *Nuovo Cimento Suppl.* **9**, 364-380, 1953.